

CHARACTERIZATION OF NANOSTRUCTURES ZnO SYNTHESIZED
THROUGH HYDROTHERMAL METHOD

WAN NUR AMALINA BINTI MIOR IDRIS

A thesis submitted in fulfillment of the requirement for the award of the Degree of
Master of Mechanical Engineering

Faculty of Mechanical and Manufacturing Engineering
Universiti Tun Hussein Onn Malaysia

JUNE 2015

ABSTRACT

ZnO nanostructures can be derived using a variety of techniques. Using hydrothermal synthesis, ZnO nanostructures can be produced easily on a large scale due to the low temperature involved. Among the factors that influence the crystallinity of ZnO nanostructures are types of alkaline solution, the alkaline pH value used and the application hours of the hydrothermal process. This research focuses on the fabricated ZnO nanostructures via hydrothermal synthesis and the effects of alkaline solution on the morphology of ZnO nanostructures. Distilled water was mixed with three types of alkaline which are NaOH, KOH and LiOH solutions in 3 different pH values. The hydrothermal process was conducted using three different time periods which are 6, 12 and 24 hours. XRD analysis was done to identify the phase and crystallinity of ZnO nanostructures. Morphology and surface roughness analysis were characterized using FESEM and AFM to observe the nanostructures growing on ZnO thin films while current against voltage testing was done to identify the resistivity of ZnO nanostructures using a 2-probe point analyzer. All of these analyses were performed on the growth of ZnO nanostructures after the hydrothermal process. The results revealed that the addition of KOH solution as a precursor provides the best nanostructure properties over other alkaline solutions. The most suitable time period required to produce the best ZnO crystalline structure is 24 hours while the perfect pH value that allows the formation of ZnO nanostructures is 12.

ABSTRAK

Umumnya, nanostruktur bagi ZnO boleh dihasilkan melalui pelbagai teknik. Melalui kaedah hidrotermal, nanostruktur bagi ZnO boleh dihasilkan dengan banyak dan prosesnya ringkas kerana melibatkan penggunaan suhu yang rendah. Antara faktor yang mempengaruhi pertumbuhan nanostruktur ZnO yang baik ialah penambahan jenis larutan alkali, kepekatan pH alkali yang digunakan dan juga masa proses hidrotermal dijalankan. Kajian ini menumpu kepada fabrikasi nanostruktur bagi ZnO melalui kaedah hidrotermal dan kesan pengaruh larutan alkali keatas morfologi kerajang nipis Zn. Air suling telah dicampur bersama 3 jenis alkali yang berbeza yang mana mempunyai 3 kepekatan pH yng berbeza. Kerajang Zn telah dijalankan proses hidrotermal selama 6, 12 dan juga 24 jam. Analisis XRD dijalankan bagi mengetahui fasa dan kehabluran bagi nanostruktur yang terhasil. Analisis morfologi dan juga analisis kekasaran permukaan yang dijalankan oleh FESEM dan AFM bertujuan untuk melihat struktur nano ZnO yang terhasil pada kerajang Zn. Ujian arus melawan voltan yang dijalankan oleh *2-point probe* bertujuan untuk mengetahui nilai keringtangan yang wujud bagi nano struktur ZnO. Kesemua analisis ini dijalankan pada kerajang ZnO selepas proses hidrotermal dijalankan. Larutan alkali yang menghasilkan nanostruktur ZnO yang baik adalah larutan alkali jenis KOH. Manakala masa yang terbaik untuk menghasilkan struktur hablur pada kerajang ZnO ialah sebanyak 24 jam dan kepekatan alkali yang sesuai digunakan adalah pH 12.

CONTENTS

	TITLE	i
	DECLARATION	ii
	DEDICATION	iii
	ACKNOWLEDGEMENT	iv
	ABSTRACT	v
	ABSTRAK	vi
	CONTENTS	vii
	LIST OF TABLES	ix
	LIST OF FIGURES	x
	LIST OF SYMBOLS	xv
	LIST OF APPENDICES	xvi
CHAPTER 1	INTRODUCTION	1
	1.1 Background of Study	1
	1.2 Statement of Problem	2
	1.3 Objectives	2
	1.4 Scope of Study	2
CHAPTER 2	LITERATURE REVIEWS	4
	2.1 Introductions	4
	2.2 Hydrothermal Synthesis	6
	2.3 Effects of Different Alkaline	8
	2.4 Effects of Different Hours	16
	2.5 Effects of Different pH	23
CHAPTER 3	METHODOLOGY	33
	3.1 Introduction	33
	3.2 Flow Chart of Research	33
	3.3 Materials Preparation	35
	3.3.1 Preparation of Zn Foil	35

3.4	Hydrothermal Process	36
3.5	Sample Analysis	37
3.5.1	X-ray Diffractometer (XRD)	37
3.5.2	Field Emission Scanning Electron Microscopy (FESEM)	38
3.5.3	Atomic Force Spectroscopy (AFM)	39
3.5.4	2-point Probe	40
CHAPTER 4	ANALYSIS AND DISCUSSION	41
4.1	Analysis and Discussion	41
4.1.1	Morphological Analysis	41
4.1.2	Crystallinity and Phase Analysis	47
4.1.3	Surface Roughness Analysis	52
4.1.4	Current against Voltage Measurement	58
CHAPTER 5	CONCLUSION	61
5.1	Conclusion	61
5.2	Recommendations	62
	REFERENCES	63
	APPENDICES	

LIST OF TABLES

2.1	ZnO nanostructured properties	6
2.2	Summary of the test using different alkaline (XRD, I-V Measurement, AFM and FESEM)	15
2.3	Results of ZnO particle sizes without surfactant in variables of times and temperatures	16
2.4	Values of I_{SC} and V_{OC} for devices of various types ITO thin films	20
2.5	Summary of tests done with different variations in time (XRD, I-V Measurement, AFM and FESEM)	22
2.6	Cell parameter of the ZnO powder based difference pH	27
2.7	Summary of tests using different pH levels (XRD, I-V Measurement, AFM and FESEM)	32
4.1	Types of nanostructures found on ZnO produced via hydrothermal synthesis.	46
4.2	Planes and Phases for first strong diffraction of ZnO nanostructures by XRD analysis	51
4.3	Values of Average Surface Roughness (Ra) and Root Mean Square Roughness (Rq) for ZnO thin films.	52
4.4	Results for the electrical properties of ZnO samples which underwent the hydrothermal process.	58

LIST OF FIGURES

2.1	Band Position of Several Semiconductor in Aqueous Electrolyte at pH 1	5
2.2	The shaped controlled synthesis of ZnO using microwave hydrothermal	7
2.3	XRD patterns of ZnO synthesized by NaOH, LiOH and NH ₄ OH alkaline solutions	8
2.4	XRD pattern for oxidation of Zn substrate by distilled water	9
2.5	Current density against voltage	10
2.6	Linear graph for ZnO thin film	10
2.7	The linear I-V curve for ZnO nanorod structures	11
2.8	AFM results for surface roughness on ZnO	12
2.9	AFM analysis for nanospherical structure for ZnO thin film using chemical bath synthesis	12
2.10	(a): FESEM of nanorods of ZnO with NH ₃ ·H ₂ O (b): FESEM of nanorods of ZnO with NH ₃ ·H ₂ O and NaOH	13
2.11	Cu-ZnO structures from FESEM for different alkaline solution (a) KOH solution (b) NaOH solution	14
2.12	FESEM image for ZnO nanorods using atomic layer deposition technique	14
2.13	XRD pattern for (I) before hydrothermal (II) after hydrothermal	17

2.14	XRD patterns of ZnO powder that prepared at (a) 180°C for 6 H using NH ₄ OH (b) 180°C for 20 H using NaOH and (c) 200°C for 20 H using NaOH	17
2.15	AFM images of surface roughness for different time during the dip-coating process (a) 30 minutes (b) 60 minutes (c) 90 minutes (d) 120 minutes (e) 150 minutes.	18
2.16	AFM result of ZnO seeded on Si substrate	19
2.17	The roughness of ZnO nanostructured by sol-gel hydrothermal synthesis	19
2.18	ZnO surfaces morphologies through FESEM at different hours of hydrothermal process (a) 1 hour (b) 3 hours (c) 5 hours (faceup) (d) 5 hours (respectively)	20
2.19	ZnO nanostructured based on different time reaction by FESEM	21
2.20	The formation of ZnO structured by Hydrothermal technique in different of pH NaOH solution	22
2.21	XRD pattern for ZnO nanostructures (a) water as solvent in pH = 8 (b) water as solvent in pH = 12 (c) methanol as solvent in pH = 8 (d) water as solvent in pH = 9	24
2.22	XRD patterns for ZnO powder based on differences of pH value	25
2.23	XRD patterns of ZnO by using Citrus aurantifolia juice extract on different pH values (a) pH=5 (b) pH=7 (c) pH=9	26
2.24	I-V characteristics of ZnO powder based based on various pH values	27
2.25	AFM result for ZnO thin film prepared at pH=8 (a) before annealing	28

	(b) after annealing	
2.26	AFM images for boron-doped ZnO thin films (a) pH=5 (b) pH=5.6 (c) pH=6.2 (d) pH=6.8	28
2.27	FESEM analysis (a) water as solvent in pH = 8 (b) water as solvent in pH = 12 (c) methanol as solvent in pH = 8 (d) water as solvent in pH = 9	29
2.28	ZnO structures through FESEM in different pH (a) pH=6 (b) pH=7 (c) pH=8 (d) pH=9 (e) pH=10 (f) pH=11 (g) pH=12	30
2.29	ZnO whisker structures through FESEM by different pH value (a) pH=6.5 (b) pH=9.5 (c) pH=10.0 (d) pH=10.5	31
3.1	Sample preparation and characterization process of Zn foils	34
3.2	Zn Foils (99.99% purity)	35
3.3	pH determination for LiOH solution	36
3.4	Teflon-lined Stainless Steel Autoclave	37
3.5	Control furnace	37
3.6	X-ray Diffractometer (XRD)	38
3.7	Field Emission Scanning Electron Microscopy (FESEM)	39
3.8	AFM	39
3.9	2-point probe	40
4.1	Morphologies of ZnO nanostructures in LiOH solution (pH= 10) after different durations of the hydrothermal process.	42
4.2	Morphologies of ZnO nanostructures in LiOH solution (pH=12) after different durations of the hydrothermal process.	42
4.3	Morphologies of ZnO nanostructures in KOH solution (pH=10) after different durations of the hydrothermal process.	43
4.4	Morphologies of ZnO nanostructures in KOH solution (pH=12) after different durations of the hydrothermal process.	44

4.5	Morphologies of ZnO nanostructures in NaOH solution (pH= 10) after different durations of the hydrothermal process.	45
4.6	Morphologies of ZnO nanostructures in NaOH solution (pH=12) after different durations of the hydrothermal process.	45
4.7	XRD pattern of ZnO synthesized in same pH of NaOH at different durations of the hydrothermal process.	47
4.8	XRD pattern of ZnO synthesized in same pH of LiOH at different durations of the hydrothermal process.	48
4.9	XRD pattern of ZnO synthesized in same pH of KOH at different durations of the hydrothermal process	49
4.10	XRD pattern for different alkaline solutions at pH=10 after 24 hours of the hydrothermal process (a) NaOH solution, (b) KOH solution (c) LiOH solution	49-50
4.11	ZnO nuclei for LiOH sample that underwent the hydrothermal process for 24 hours at pH=10	50
4.12	XRD pattern for KOH solution sample in different pH value (a) pH=10 (b) pH=12	51
4.13	Sample immersed in KOH solution (pH=10) and underwent a 6-hour hydrothermal process (a) Surface roughness by AFM (b) Morphology of ZnO nanostructures by FESEM.	53
4.14	Sample immersed in LiOH solution (pH=10) and underwent a 6-hour hydrothermal process (a) Surface roughness by AFM (b) Morphology of ZnO nanostructures by FESEM.	53
4.15	Sample immersed in NaOH solution (pH=10) and underwent a 6-hour hydrothermal process (a) Surface roughness by AFM	53

	(b) Morphology of ZnO nanostructures by FESEM.	
4.16	Average Surface Roughness (<i>Ra</i>) values for KOH solution based on differences in pH values and hydrothermal process hours.	54
4.17	Average Surface Roughness (<i>Ra</i>) values for NaOH solution based on differences in pH values and hydrothermal process hours.	55
4.18	Average Surface Roughness (<i>Ra</i>) values for LiOH solution based on differences in pH values and hydrothermal process hours.	55
4.19	Surface Roughness of ZnO nanostructures after different durations of the hydrothermal process (a) 6 hours (b) 12 hours (c) 24 hours.	56
4.20	Surface roughness of ZnO thin films based on the different NaOH pH values (a) pH=6 (b) pH=12	57
4.21	Average Surface Roughness (<i>Ra</i>) for different alkaline solutions based on different pH values and hydrothermal duration.	57
4.22	Morphology of ZnO nanostructures that conducted in LiOH solution at pH 12 at different durations (a) 6 hours (b)12 hours (c) 24 hours.	59
4.23	Resistivity of ZnO nanostructures produced using hydrothermal synthesis.	60

LIST OF SYMBOLS

°C	-	Degree celcius
%	-	Percent
pH	-	Pontential Hydrogen
ZnO	-	Zinc Oxide
TCO	-	Transperent and Conductive Oxide
PL	-	Photoluminescences
ITO	-	Indium-Tin Oxide
TiO ₂	-	Titanium Dioxide
ZAH	-	Zinc Acetate Hydrate
NaOH	-	Sodium Hydroxide
KOH	-	Potassium Hydroxide
LiOH	-	Lithium Hydroxide
HCl	-	Hydrochloride
XRD	-	X-ray Diffractometer
FESEM	-	Field Emission Scanning Electron Microscopy
FTIR	-	Fourier Transform Infrared Spectroscopy
nm	-	Nanometer
EtOH	-	Ethanol
I _{sc}	-	Short Circuit Current
V _{oc}	-	Voltage-Operated Channels

LIST OF APPENDICES

A	Morphology of ZnO nanostructures by FESEM	69
B	Surface roughness of ZnO nanostructures by AFM	73
C	Crystallinity of ZnO nanostructures by XRD	77
D	Current against voltage measurement of ZnO nanostructures by 2-point Probe	81

CHAPTER 1

INTRODUCTION

1.1 Background of study

Zinc Oxide (ZnO) has a wide number of properties which has gained considerable attention from researchers over the past few years. ZnO is a popular material used in semiconductor research and this was mentioned back in 1945 (Gomez & Tigli, 2012). World-wide use of ZnO that has 9 % of metallic zinc is more than 1.2 million tonnes per year (International Zinc Association, 2011). Due to its unique chemical properties and structure, ZnO is increasingly being used in the production of electronic devices. The applications of ZnO are not only limited to the engineering field, but also the pharmaceutical industry, cosmetic and food packaging industry.

There are wide applications of ZnO in hybrid solar cells and organic solar cells due to its low cost, ease of synthesis, non-toxicity, high stability and good optoelectronic properties (Huang, Yin, & Zheng, 2011). Doped ZnO thin films are transparent electrodes for solar cells. Solar cells require a transparent and conductive oxide (TCO) thin film that can extract the electrical current and allow the light to enter the absorber layers (Tadatsugu, 2005). ZnO is not only highly transparent but also highly conductive and strongly suitable to be a TCO candidate.

There are two types of synthesis methods to obtain the ZnO nanostructure. The ways are solution phase synthesis and gas phase synthesis. For solution phase synthesis, normally the aqueous solution is used and the process is referred to as hydrothermal growth process. Baruah & Dutta(2009) in their research said that solution phase synthesis processes consist of several methods. First, Zinc Acetate Hydrate (ZAH) is derived from nano-colloidal sol-gel route, ZAH in alcoholic solutions with Sodium Hydroxide (NaOH), template assisted growth, spray pyrolysis for growth of thin films and electrophoresis. Due to the variety in methods, the

structure and look of ZnO produced could be different. The best structure of ZnO is nanowire because of its good performance in electronics, optics and photons field (Yangyang *et al.*, 2012).

1.2 Statement of Problem

Basically, ZnO nanostructures can be derived using a variety of techniques. Based on Segovia *et al.*, (2012) , hydrothermal synthesis or wet chemistry techniques are simple and proved to be efficient methods to obtain nanostructure thin films on a large scale. Besides that, Yangyang *et al.*, (2012) said that hydrothermal synthesis has been used for the synthesis of 1-D nanostructures that are useful in different fields such as Dye-Sensitized Solar Cells due the unique electrical properties. Nanostructures that are categorized in 1-D are nanowires, nanorods, nanofibres, nanobelts and nanotubes. The growth of ZnO nanostructures via hydrothermal synthesis can be controlled by alkaline reagents, initial solution pH, and growth duration. All of these parameters affect the nanostructures of ZnO and diversifies the properties of ZnO.

Research on ZnO nanostructures produced based on different parameters will be emphasized in this study. The best parameters to produce ZnO nanostructures with electrical properties based on solar cell application through hydrothermal synthesis will be identified.

1.3 Objectives

- 1) To fabricate the nanostructure of ZnO via hydrothermal synthesis method.
- 2) To study the effects of different types of alkaline solution on the morphologies of the synthesized ZnO nanostructures.

1.4 Scope of Study

- 1) Zinc foil (99.9% purity) was used as substrate and solid reagent.
- 2) Zinc foils were produced via hydrothermal synthesis in different alkaline solutions such as NaOH, KOH and LiOH.
- 3) Hydrothermal synthesis by an autoclave at 120°C for 6, 12 and 24 hours.

- 4) Alkaline concentrations of pH 10 and 12 were used for formation control of ZnO nanostructure.
- 5) The crystallinity and phases of ZnO nanostructures were characterized by X-ray Diffractometer (XRD).
- 6) Surface morphology of the ZnO nanostructures with different alkaline concentration was characterized by Field Emission Scanning Electron Microscopy (FE-SEM).
- 7) The surface roughness of ZnO nanostructures was measured by Atomic Force Microscopy (AFM).
- 8) 2-point probe was used to measure the current-voltage (I-V) for ZnO nanostructures.

CHAPTER 2

LITERATURE REVIEW

2.1 Introductions

Thin films are very thin layers of substances that are used to support materials. It is common in solar energy applications today to generally use thin films on solar panels to absorb energy from the sun. To do so, the photovoltaic material will be deposited in thin layers on substrates such as glass, plastic or metal. Thin film solar cells have several differences as compared to traditional solar cells like silicon whereby it performs as a semi-conductor. Thin films are considered second generation solar cells after silicon solar cells because they are made from semiconductor materials that are a few micrometers in thickness.

Thin films will be deposited on various materials to produce nanostructures. The application of nanoscale materials will be able to convert solar energy with higher efficiency and produce low-cost devices (Beard, Luther, and Nozik, 2014). This indirectly revolutionises solar cell application. Nanostructures layered on thin film have several advantages. Based on the review made by Sagadevan (2013), there are three advantages of nanostructures in solar energy application. First advantage being, the absorption of nanostructures are more effective than the absorption of actual film thickness due to multiple reflections. Secondly, the electrons generated by light travels a much shorter path avoiding losses. Lastly, the size of nanoparticles allows more flexibility in the absorption of solar cells.

ZnO polar surfaces are actually very stable and include many different nanostructures. The nanostructures provide many advantages for several applications, especially for catalyses and surfaces. The surface is easier to modify and provides improved solar cell performance when it is running (Chou *et al.*, 2007). ZnO also has a band gap that is the same as TiO₂ while having much higher electron

mobility. Figure 2.1 shows a band position of several semiconductors in aqueous electrolyte at pH 1. The greater gap allows higher breakdown voltage and larger ability to sustain electric fields (Baruah and Dutta, 2009).

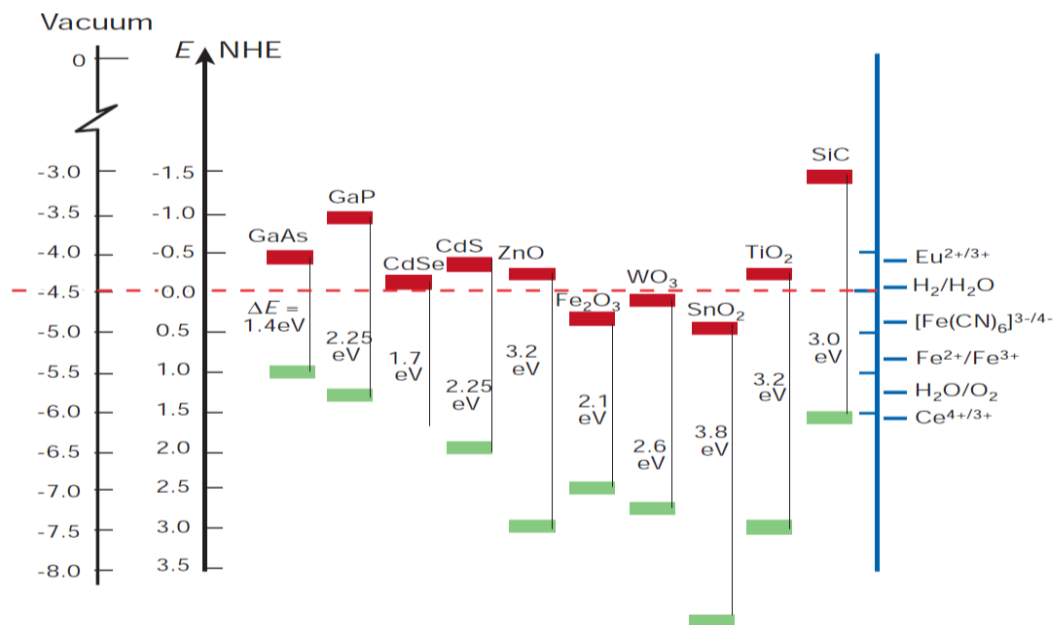


Figure 2.1: Band Position of Several Semiconductor in Aqueous Electrolyte at pH 1 (Chou *et al.*, 2007)

One dimensional nanostructure of ZnO is more efficient to carry and transport with decreased surface defects, grain boundaries, disorders, and discontinuous interfaces (Chen *et al.*, 2010). ZnO also has properties like transparent conducting oxides (TCO). Usually, the most widely used TCO is indium-tin oxide (ITO). However, an active search for alternative materials is underway because of the high processing cost. The applications of ZnO as TCO is well-suited because of its low cost and non-toxicity (Noriega *et al.*, 2010). Thus, it makes a popular TCO in the application of solar cells. It is widely used in applications of solar cells because of their optical transmission in the visible and electrical conductivity. Ridhuan *et al.*, (2012) in their paper said that, the seeding of substrates by hydrothermal method has better controlled morphology and growth direction of ZnO nanostructures. Table 2.1 shows the ZnO nanostructured properties.

Table 2.1: ZnO nanostructures properties (Fan & Lu, 2005)

Properties	Values
Lattice Parameters (T= 300K)	a=b=3.25 Å c=5.21 Å u=0.348 c/a=1.593-1.6035
Density	5.606 gm/cm ³
Melting Point	2248 K
Stable Crystal Structure	Wurtzite
Dielectric Constant	8.66
Refractive Index	2.008
Band Gap (E _g)	3.37 eV (direct)
Exciton Binding Energy	60 meV
Electron/ Hole Effective Mass	0.24 m _o / 0.59 m _o
Hole Mobility (300K)	5-50 cm ² /Vs
Electron Mobility (300K)	100-200 cm ² /Vs

2.2 Hydrothermal Synthesis

Hydrothermal synthesis is the technique of fabricating materials from low temperature aqueous solution in high vapour pressure and a synthesis process of single crystals. This method will save energy and is more environmental-friendly because the reaction is done in closed system conditions. Moreover, this synthesis is also able to fabricate single crystals in low temperatures. The main advantage of synthesising in low temperatures is that it is simple and energy efficient (Komarneni, 2003). To control the size and shape of the nanophases, this method is more suitable.

Hydrothermal synthesis can be done through two methods: Conventional Hydrothermal and Microwave Hydrothermal. Conventional Hydrothermal synthesis uses cold seal vessels and Parr vessels. Cold seal vessels control pressure and temperature, while Parr vessels only control temperature with precision. Parr vessels will not control the pressure parameters. Hydrothermal process by microwave however, gives other advantages when compared to conventional hydrothermal method. Komarneni (2003) in his study said, reaction system by microwave has more rapid kinetics than conventional hydrothermal. The rutile crystallisation happens in between 0.5 to 2 hours in 0.5 to 3 M titanium oxychloride solutions, while the reaction through conventional hydrothermal takes 3 days to be completed.

In a study done by Kharisov, Kharissova, and Méndez (2012), they showed the morphology control of ZnO nanostructures by microwave hydrothermal. ZnO nuclei will transform into nanorods by preferential c-axis [002] with oriented 1D growth. Nanowires that form from nanorods become nanospindles because of the

increase in diameter and local dissolution. The nanorods can also become nanodendalions from the multiple growths of nanorods. Crystal growth along the [002] direction becomes nanoslices due to quasi 1D growth. Finally, nanotruster vanes form due to assembled growth of nanoslices. Figure 2.2 shows the shape-controlled synthesis of ZnO nanorod, nanowire, nanotruster vanes, nanodendalions and nanospindles using the microwave hydrothermal method.

From the researches done, we now know that ZnO materials do have important properties like photoluminescence and photocatalysis. The nanostructures that give good performances in photoluminescence are known as nanoflowers (Lai *et al.*, 2011). This structure is a special three dimensional nano-ZnO. Between the variables that can be controlled to develop good nanostructures are: types of alkaline solution, temperature, hydrothermal reaction time, and difference in pH value.

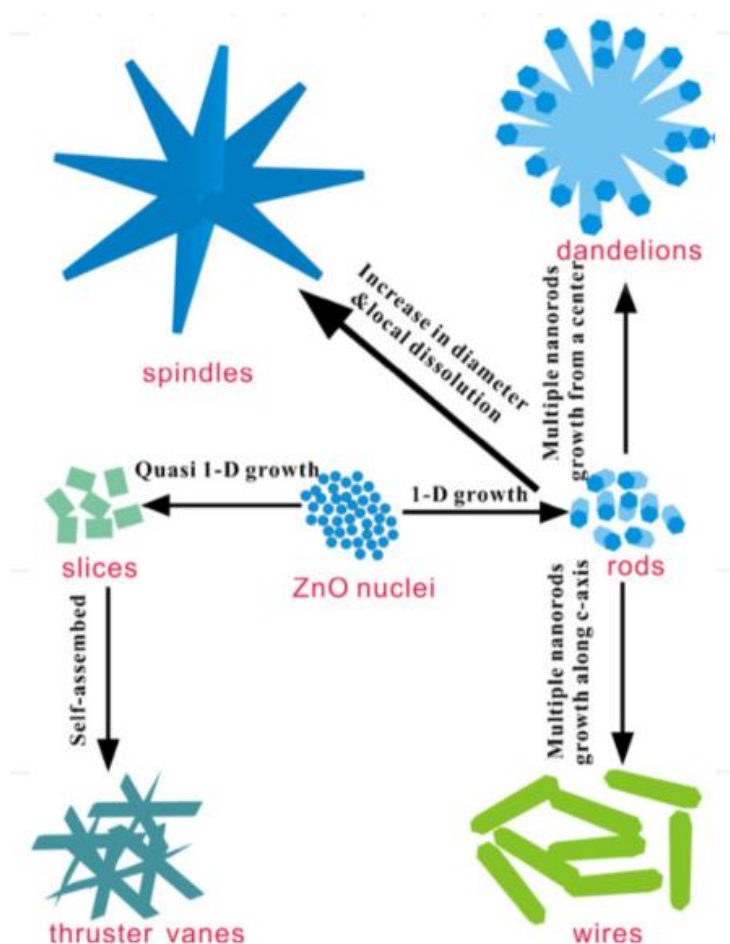


Figure 2.2: The shaped controlled synthesis of ZnO using microwave hydrothermal (Kharisov *et al.*, 2012)

2.3 Effects of Different Alkaline

The use of different alkaline solution in hydrothermal synthesis will give a result that is non-toxic, environmentally beneficial, easily available, and relatively inexpensive chemical. In the research by Ekthammathat *et al.*, (2014), it shows that alkaline solution helps in the crystallisation process and generate nanostructure like rod, pencil and star. The ZnO is synthesised by NaOH, LiOH and NH₄OH. Using these alkaline solutions result in a ZnO thin film that is very sharp in XRD pattern which indicates that product has good crystalline structure. Figure 2.3, shows that all diffraction patterns can be categorised as hexagonal wurtzite structures. ZnO that is synthesised in NaOH solution has the highest diffraction peak at 34.45°. However, ZnO synthesized using LiOH and NH₄OH solutions do have strong diffraction peaks on (002) and (101) planes in relatively intensified diffractions.

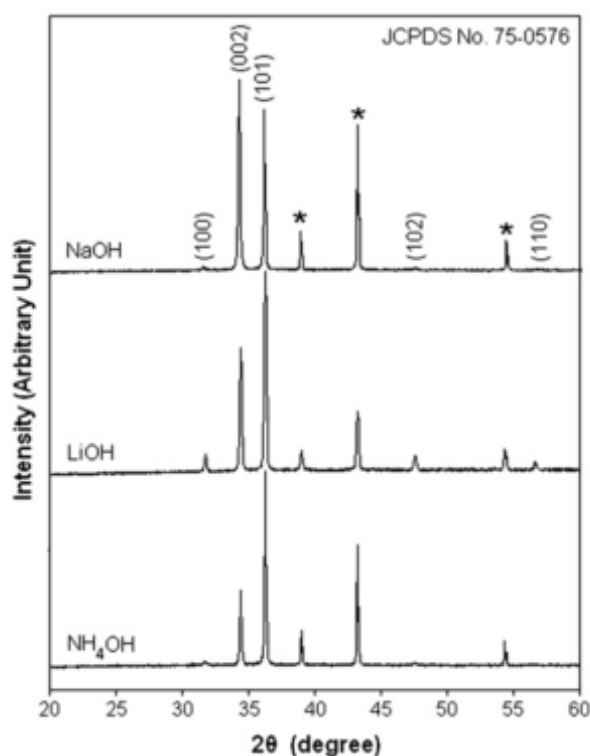


Figure 2.3: XRD patterns of ZnO synthesized by NaOH, LiOH and NH₄OH alkaline solutions (Ekthammathat *et al.*, 2014).

Ni *et al.*, (2005) also conducted a research on the preparation of ZnO nanorods that grows in powder form. In his research, KOH solution was mixed with ZnCl₂ to produce the ZnO powder through the hydrothermal process. The result of

XRD shows a strong diffraction peak at (101) plane and it directly shows that this material has good crystallinity and size. By using KOH solution, the sizes of the structures become more homogeneous and have a mean size of about 50 nm x 250 nm.

Based on the study by Pei *et al.*, (2010) on oxidation of Zn substrate by distilled water however, the highest peak of intensity by XRD are also shown on planes (101) and (002). The strong diffraction peaks on the planes were suggested to have a preferential growth direction even through the use of distilled water as precursor. The XRD pattern is shown in Figure 2.4.

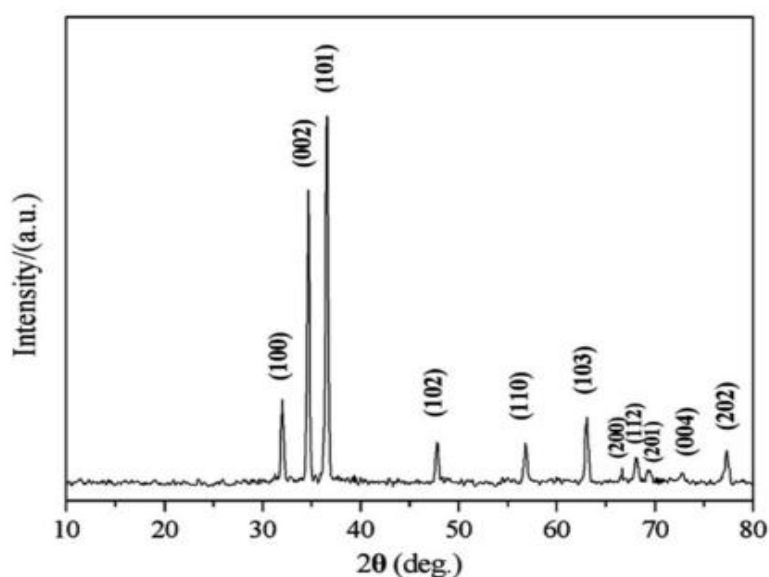


Figure 2.4: XRD pattern through oxidation of Zn substrate by distilled water (Pei *et al.*, 2010)

The use of a variety of alkaline as precursor is able to give different thickness in ZnO layer growths. The thicker the ZnO layers might be due to the low value of conversion efficiency. This statement is based on the study conducted by Baviskar, Tan, Zhang, and Sankapal (2009), where the value of voltage is 428 mV and the photovoltaic conversion efficiency is 0.34 %. Figure 2.5 shows the result of current density against voltage (J-V) from the study. Besides that, it is also found that the thickness value is indirectly caused by the increase of the resistivity (Shariffudin, Salina, Herman, and Rusop, 2012).

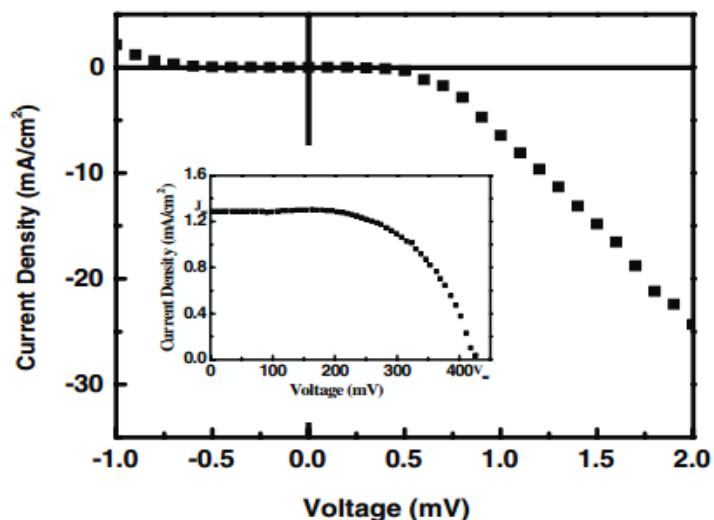


Figure 2.5 : Current density against voltage (Baviskar *et al.*, 2009)

The research from Mondal, Kanta, and Mitra (2012) on ZnO film deposition on a microscope glass as substrate shows that the sample has ohmic character from the current-voltage plotted below. The deposition process of ZnO on microscope glass is done by having the chemical dipping solution added with Ammonium Hydroxide (NH_4OH) in water. Based on Figure 2.6, the plotting graph of current against voltage is linear. It shows that the ZnO is an ohmic material.

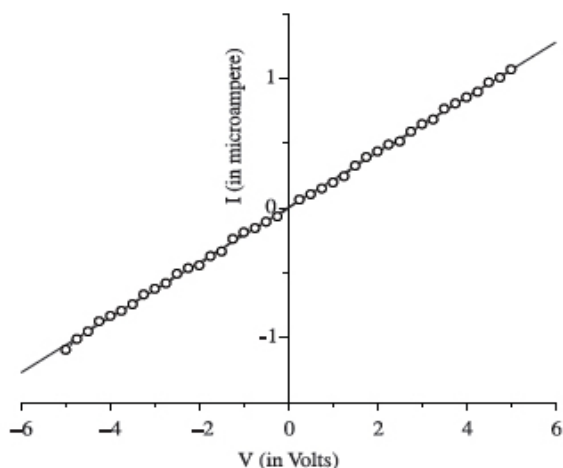


Figure 2.6: Linear graph for ZnO thin film (Mondal, Kanta, and Mitra, 2012)

The experiment by Choi *et al.*, (2010) also shows the result of ZnO-Ag interface as an ohmic character. This is because there is no electron energy barrier occurring at the interface and the value is 4.5 eV, as show in Figure 2.7. ZnO nanorods are a substrate on a flexible polyethersulfone (PES) and were then prepared

by using hydrothermal synthesis. The solution that is use in this experiment is NaOH and Zinc acetate dehydrate. ZnO nanorods is the third layer on the PES substrate while the first and second layer are Ti and Ag layers. These layers are applied using spin coating techniques.

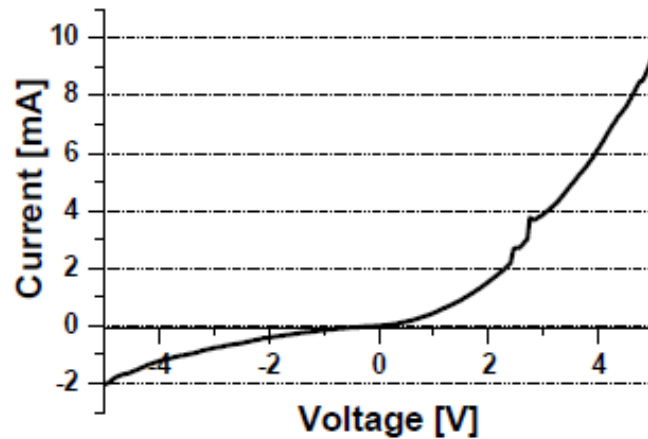


Figure 2.7: The linear I-V curve for ZnO nanorod structures (Choi *et al.*, 2010)

In the research by Vijayan *et al.*, (2008) the application shows the deposition of ZnO on glass substrate by dipping it in NaOH and Zinc Sulphate (ZnSO_4) solutions results in surface roughness on the films over an area of $20 \times 20 \mu\text{m}^2$ when in contact. This result is shows in Figure 2.8. The ZnO thin film was then immersed in alkaline zinc nitrate to grow the nanostructures on the glass substrate. While in the research by Shinde, Gujar, and Lokhande (2007), they used chemical methods to make the ZnO layer on the glass substrate. The structure that is grown on the substrate can be categorised as nanospherical because it has uniform spherical grains in an average size of $\sim 400\text{nm}$. The surface roughness of this sample was analysed by AFM as shown in Figure 2.9.

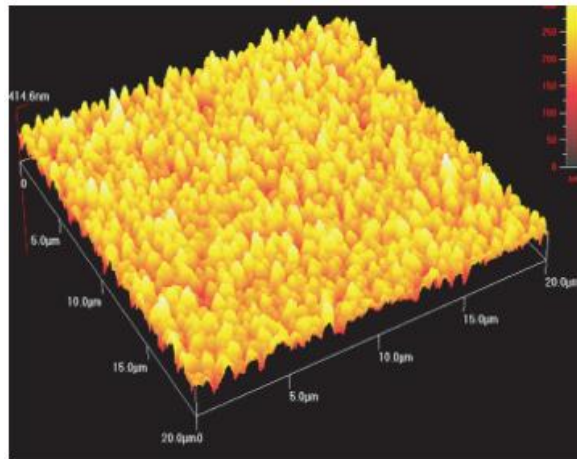


Figure 2.8: AFM results on surface roughness on ZnO (Vijayan *et al.*, 2008)

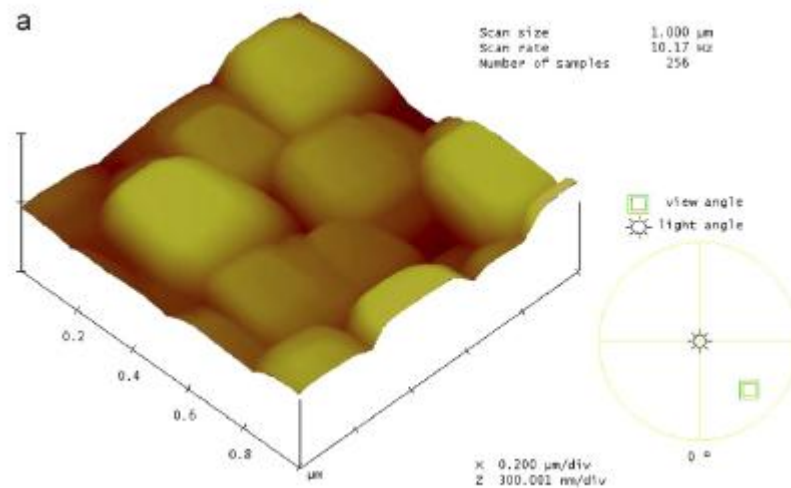


Figure 2.9: AFM analysis of nanospherical structures for ZnO thin film using chemical bath synthesis (Shinde *et al.*, 2007)

Meanwhile, the research from Yang *et al.*, (2008), demonstrated the synthesis of ZnO with NaOH and $\text{NH}_3\cdot\text{H}_2\text{O}$ solution at 60°C for 7 days in autoclave. The result is a densely packed array of nanorods with diameter ranging between 50 nm until 200 nm and has a length of over than $10\ \mu\text{m}$. ZnO that is synthesised using $\text{NH}_3\cdot\text{H}_2\text{O}$ with NaOH solution can grow the nanorods longer in length and sharper in tips if compare with ZnO nanostructure synthesis by (a) ZnO that is diluted in $\text{NH}_3\cdot\text{H}_2\text{O}$ and (b) ZnO diluted in $\text{NH}_3\cdot\text{H}_2\text{O}$ and NaOH using FESEM.

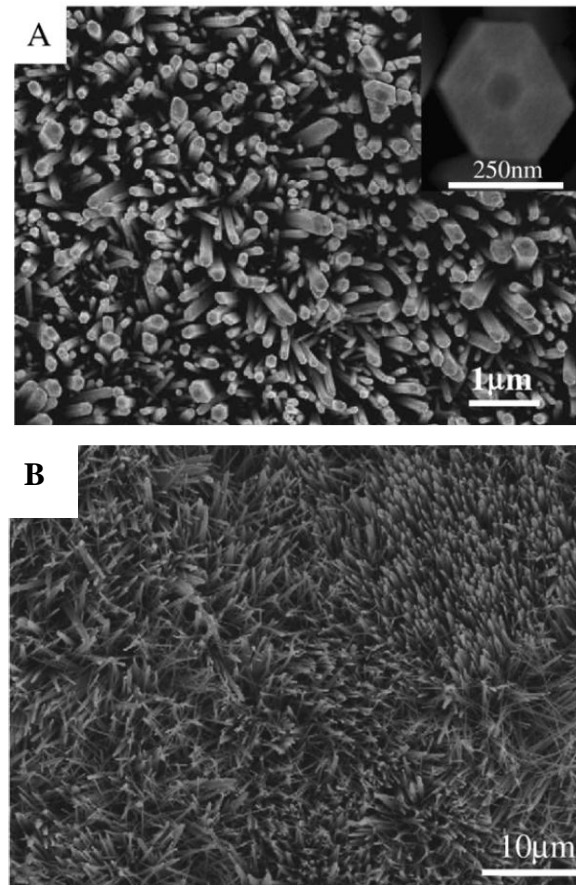


Figure 2.10 (a): FESEM of nanorods from ZnO with $\text{NH}_3 \cdot \text{H}_2\text{O}$ (b): FESEM of nanorods from ZnO with $\text{NH}_3 \cdot \text{H}_2\text{O}$ and NaOH (Yang *et al.*, 2008)

Studies by Dezfoolian, Rashchi, and Ravanbakhsh (2014), on Cu-ZnO nanostructured based anodisation technique, reports that there were nano-flower structures spotted. The pure brass was anodised by KOH and NaOH solution in different concentrations. The different types of alkaline caused the difference in growth of the Cu-ZnO structures. The difference in structures can be seen in Figure 2.11. The structure from the NaOH solution causes more nano-flowers structures to grow compared to the application of KOH solution.

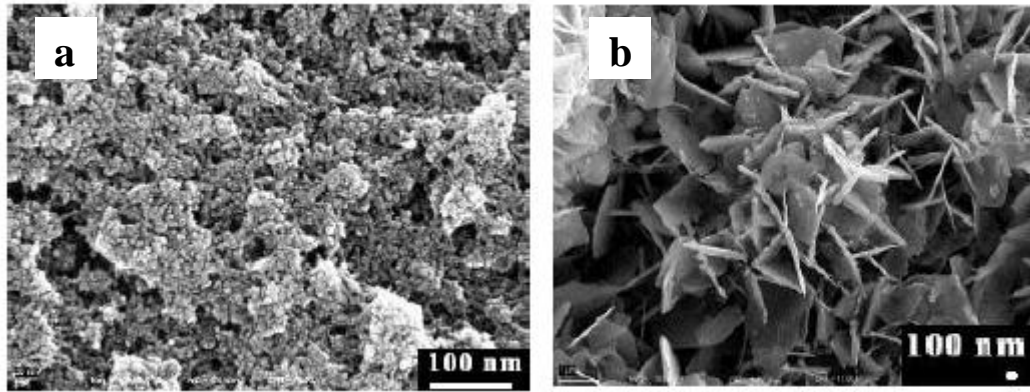


Figure 2.11: Cu-ZnO structures from FESEM for different alkaline solution (a) KOH solution (b) NaOH solution (Dezfoolian *et al.*, 2014)

However, it is also found that, using weak alkali precursor will also produce ZnO nanostructures. This statement was proven through the study conducted by Li *et al.*, (2007) which used ammonia as the precursor to produce ZnO nanostructures. In the experiment by Zhang *et al.*, (2013), it showed ZnO nanostructures grown using the atomic layer deposition process, which resulted in nanorod structures forming in the structure of ZnO shown in Figure 2.12. The formation of ZnO nanorod structures is a result from the immersion of the ITO substrate in zinc nitrate hexahydrate and hexamethylenetetramine. Hexamethylenetetramine is a weaker alkaline than ammonia. Table 2.2 shows the summary of references used in this literature review section.

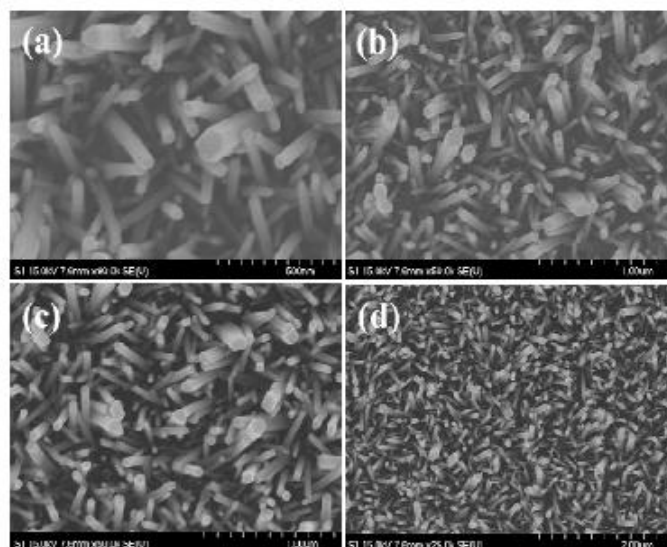


Figure 2.12: FESEM image for ZnO nanorods using atomic layer deposition technique (Zhang *et al.*, 2013)

Table 2.2: Summary of the test using different alkaline (XRD, I-V Measurement, AFM and FESEM)

XRD		
Researchers	Parameter	Results
Ekthammathat <i>et al.</i> , (2014)	Method : Hydrothermal Solution : NaOH, LiOH and NH ₄ OH	Plane: (002) and (101)
Pei <i>et al.</i> , (2010)	Method : Hydrothermal Solution: Distilled water	Plane: (101) and (002)
Ni <i>et al.</i> , (2005)	Method: Hydrothermal Solution: ZnCl ₂ and KOH	Plane : (101)
AFM		
Researchers	Parameter	Results
Vijayan <i>et al.</i> , (2008)	Method :Double Dip Solution : NaOH (first dip) and hot water (second dip)	Figure 2.8
Shinde <i>et al.</i> , (2007)	Method: Immersed in chemical Solution: Ammonia	Figure 2.9
Solar Simulator		
Researchers	Parameter	Results
Baviskar <i>et al.</i> , (2009)	Method : Wet Chemical Solution : Zinc Acetate (CH ₃ COO) ₂ Zn 2H ₂ O, Hexamethylene tetraamine (HMTA) (CH ₂) ₆ N ₄ and Ammonia (NH ₃)	Figure 2.5
Mondal <i>et al.</i> , (2012)	Method: Chemical Dipping Solution: Water (H ₂ O) and Ammonia Hydroxide (NH ₄ OH)	Figure 2.6
Choi <i>et al.</i> , (2010)	Method: Hydrothermal Solution: NaOH and zinc acetate dehydrate	Figure 2.7
FESEM		
Researchers	Parameter	Results
Yang <i>et al.</i> , (2008)	Method : Hydrothermal Solution : NH ₃ H ₂ O and NaOH	Figure 2.10
Dezfoolian <i>et al.</i> , (2014)	Method: Anodization Solution: KOH and NaOH	Figure 2.11
Zhang <i>et al.</i> , (2013)	Method: Atomic Layer Deposition Solution: zinc nitrate hexahydrate and hexamethylenetetramine	Figure 2.12

2.4 Effects of Different Hours

According to a review by Kołodziejczak-Radzimska & Jesionowski, (2014) on ZnO synthesis, they said that the increase in diameter of ZnO particles were based on the increased time of the hydrothermal process. Ismail *et al.*, (2005) also conducted ZnO synthesis using hydrothermal method in his research. In his research, the $\text{Zn}(\text{CH}_3\text{CO}_2)_2 \cdot 2\text{H}_2\text{O}$ were mixed with NaOH and hexamethylenetetramine using magnetic stirring at room temperature. $\text{Zn}(\text{OH})_2$ formed and was treated using hydrothermal process. The hydrothermal process was conducted from 5 to 10 hours and at temperatures of 100°C to 200°C. Table 2.3 shows the result of the experiment without the use of any surfactant.

Table 2.3: Results of ZnO particle sizes without surfactant in variable times and temperatures (Ismail *et al.*, 2005).

Sample	Time (hours)	Temperature (°C)	Particle size (nm)
R5	5	150	60
R7	10	150	83
R9	7.5	100	55
R11	7.5	200	82

The result shows that the variation in time affected the ZnO particle sizes more as compared to the variation in temperature. However, the research by Zou *et al.*, (2014) found that the shorter the time given to hydrothermal process causes the XRD patterns to have less peaks and the intensity of the peaks were not high. In the research by Shi, Gao, & Xiang, (2010), however shows there is a difference between the before and after using hydrothermal process. The difference can be observed from the XRD patterns in Figure 2.13. The XRD patterns after hydrothermal process are more intense compared to the XRD patterns before hydrothermal process. This happens because the samples that had undergone hydrothermal process have formations of nanostructures.

From the research by Nagaraju *et al.*, (2010), the ZnO powder was synthesised by hydrothermal process in various temperatures and time with addition of NaOH as well as NH_4OH solution. The formation of nanorods from the ZnO powder is from the reaction with the NaOH and NH_4OH solution during hydrothermal process. Figure 2.14 shows no difference between the XRD patterns

although hydrothermal process was done in a variety of parameters. All the samples have the highest intensity at plane (101). Besides that, the XRD pattern also shows that ZnO powder has a crystalline structure at plane (002) and (100) due the peaks that occur in the XRD patterns.

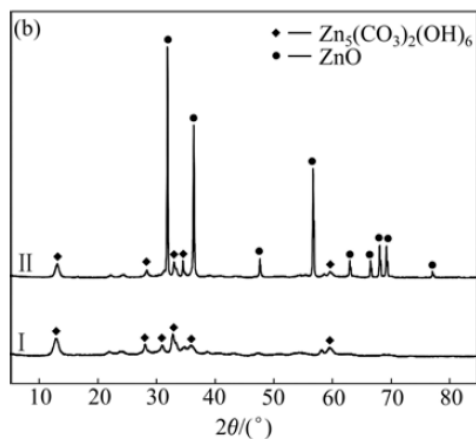


Figure 2.13: XRD pattern for (I) before hydrothermal (II) after hydrothermal (Shi *et al.*, 2010)

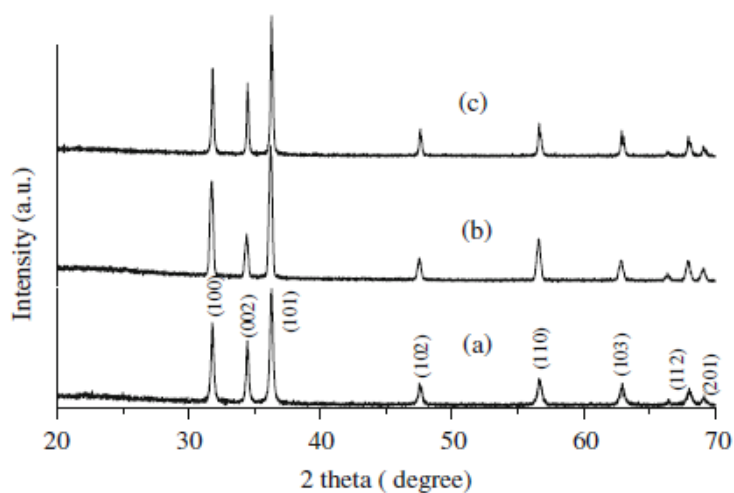


Figure 2.14:z XRD patterns of ZnO powder that was prepared at (a) 180°C for 6 H using NH_4OH (b) 180°C for 20 H using NaOH and (c) 200°C for 20 H using NaOH (Nagaraju *et al.*, 2010)

Based on the experiment by Nithya & Radhakrishnan, (2012) the surface roughness for thin film decreased with the increase in thickness of ZnO deposition. The increased thickness of ZnO deposition layers with various times are shown in Figure 2.15 .This experiment was conducted with different coating times. The substrate was dipped in Ammonium (NH_4^+) solution that was maintained at pH 9.

The longest time for this dip-coating process is 150 minutes and the shortest time is 30 minutes. The thickness of ZnO deposition for the longest time is 161.267 nm while for the shortest time is 25.321 nm.

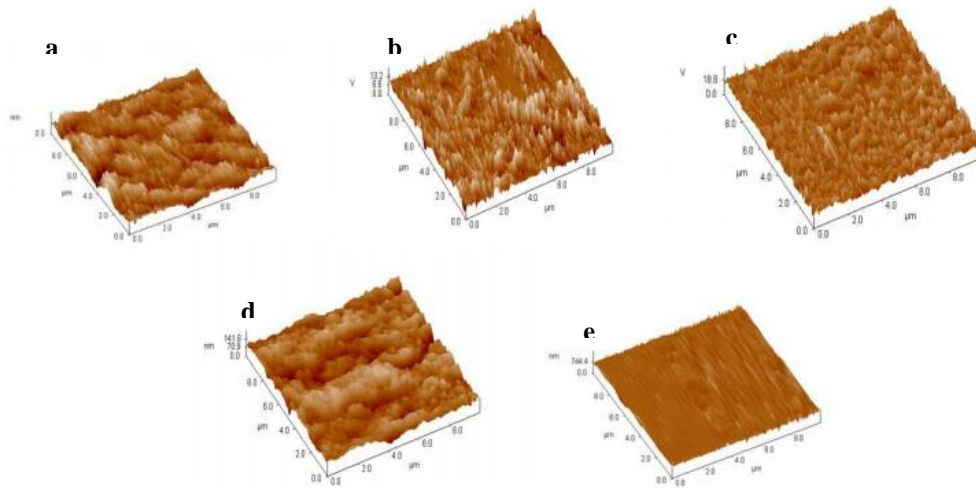


Figure 2.15 : AFM images of Surface Roughness for different times during the dip-coating process (a) 30 minutes (b) 60 minutes (c) 90 minutes (d) 120 minutes (e) 150 minutes. (Nithya & Radhakrishnan, 2012)

In the experiment on ZnO conducted through hydrothermal synthesis, ZnO nanowires displayed growth that is uniform in size of about 20-30 nm (Zhitao, Sisi, Jinkui, & Yong, 2013). Figure 2.16 shows the AFM image for this sample. This ZnO sample was deposited on Si and underwent hydrothermal synthesis for 1-12 hours at 95°C after the sol-gel process and spin-coating technique. Based on the experiment that was conducted by Kamaruddin *et al.*, (2010) on ZnO nanostructures growth by sol-gel hydrothermal, the surface of the sample was rougher. However, the sample is still categorized as nanostructures based on Figure 2.17. This sample was underwent sol-gel hydrothermal method for 5 hours at 95°C.

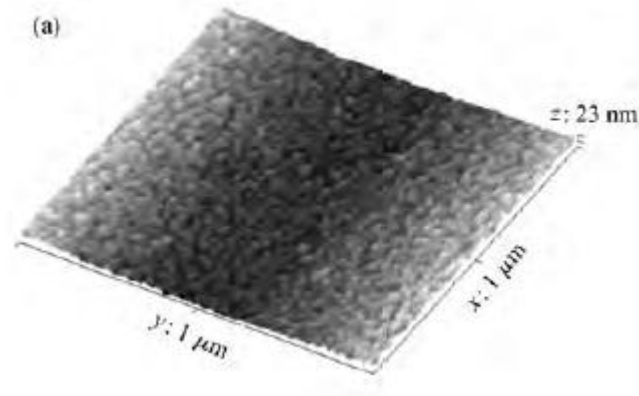


Figure 2.16: AFM results of ZnO seeded in Si substrate (Zhitao *et al.*, 2013)

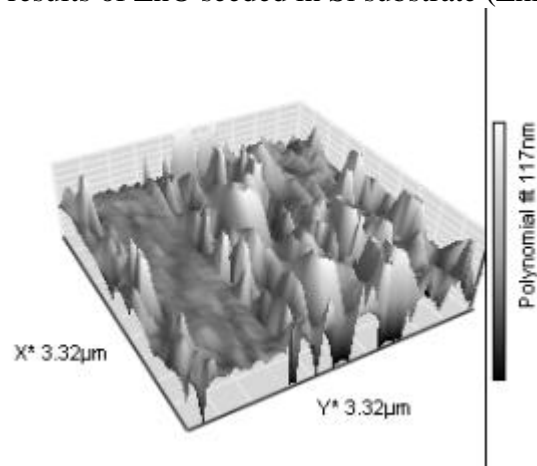


Figure 2.17: The roughness of ZnO nanostructures by sol-gel hydrothermal synthesis (Kamaruddin *et al.*, 2010)

Through the research that was conducted by Amin & Willander, (2012) the value of voltage was extracted at 1.52 V. In this experiment, the CuO was layered on a ZnO substrate with ITO and was held in a hydrothermal synthesis for 6-8 hours at 50°C. The voltage value of 1.55 V was a close approximate to the experiment voltage value conducted by Baek & Tuller, (1995).

ZnO was able to reach its best value from the current density (I_{sc}) through the performance of the devices after 20 minutes as compared to other types of hybrid solar cell. This was stated in Lira-Cantu & Krebs, (2006) paper on the performance of thin film semiconductor oxides. Other thin films that were tested in this study besides ZnO is TiO_2 , Nb_2O_5 , CeO_2 , and CeO_2-TiO_2 . All this thin films were prepared using sol-gel solution that was coated on ITO substrates through the spin coating method. Table 2.4 shows the values of I_{sc} and V_{oc} for devices of various types of ITO thin films.

Table 2.4: Values of I_{SC} and V_{OC} for devices of various types of ITO thin films (Lira-Cantu & Krebs, 2006)

Oxide	Initial (st start)		From IV curve		Maximum I_{SC} (mA/cm ²)	FF (%)
	V_{OC} (V)	I_{SC} (mA/cm ²)	V_{OC} (V)	I_{SC} (mA/cm ²)		
TiO ₂	-0.74	+0.39	-0.70	+0.16	+0.17	25
Nb ₂ O ₅	-0.22	+0.04	-0.42	+0.27	+0.13	30
ZnO	-0.39	+0.11	-0.46	+0.17	+0.21	37
CeO ₂ -TiO ₂	+0.42	-0.007	-	-	+0.08	32
CeO ₂	+0.12	-0.004	-	-	+0.06	25

From the experiment done by Chen *et al.*, (2014), the nanostructures grown on the ZnO samples were synthesized using hydrothermal method with distilled water. The hydrothermal process was conducted at 100°C for 1, 3, and 5 hours. Figure 2.18 shows the ZnO morphology through FESEM. The morphology after 1 hour of hydrothermal shows no formation of nanorods or nanoflowers and only irregular-plate structure growth. Liu *et al.*, (2005) however, has stated that the different morphology occurs with different substrates. Furthermore, the time span of deposition will also influence the structure's growth.

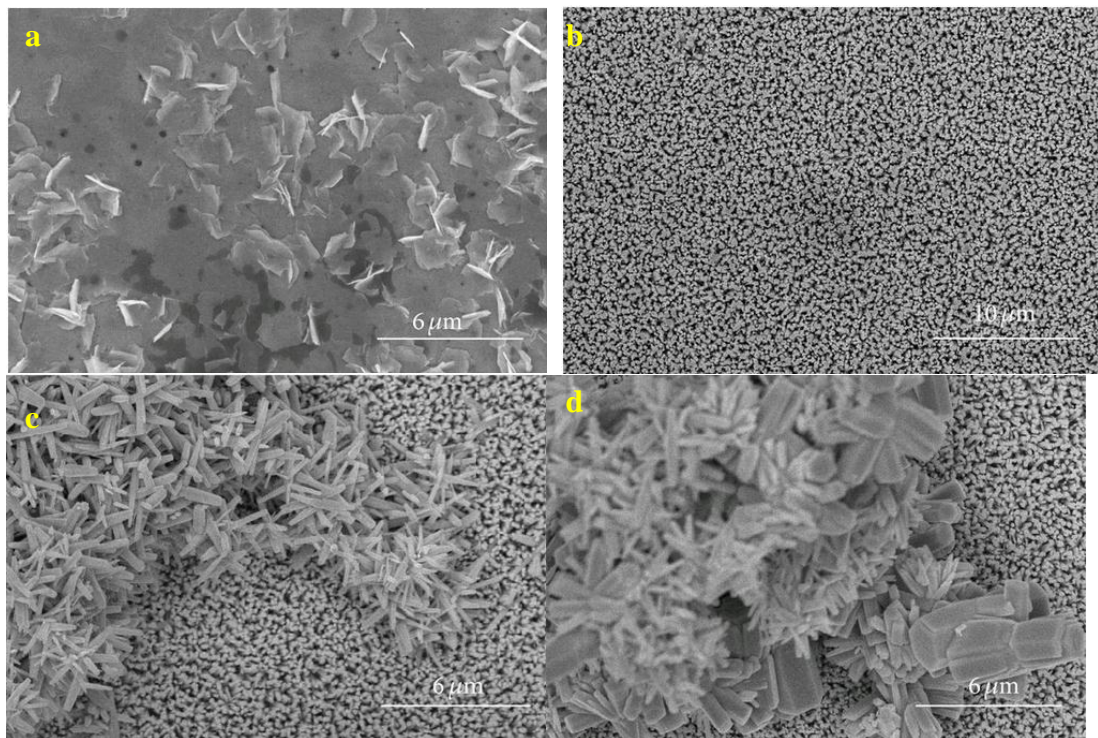


Figure 2.18: ZnO surface shows morphologies through FESEM at different hours of hydrothermal process (a) 1 hour (b) 3 hours (c) 5 hours (faceup) (d) 5 hours (respectively) (Liu *et al.*, 2005)

In the research by Haque *et al.*, (2012) on nanostructures of ZnO thin films using the uncovered hydrothermal method, it is charted that they ran the experiment for 60, 120 and 240 minutes. The formation of ZnO nanostructures were then analysed through FESEM. Figure 2.19 shows the differences of ZnO nanostructures based on the differences in hydrothermal times. Based on the figure, it is clearly shown that the hexagonal structure formed at the 4 hour mark during the hydrothermal process. Table 2.5 shows the summary of tests done with variations in time allocations with results from XDR, FESEM, I-V measurement and AFM.

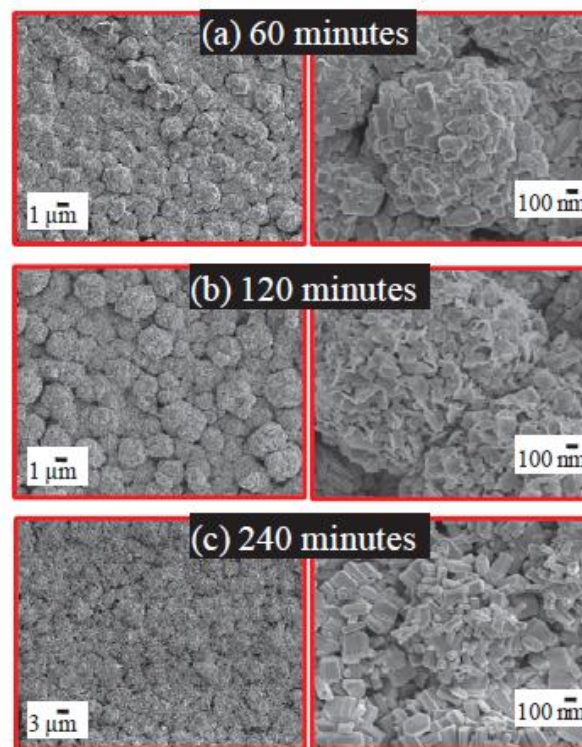


Figure 2.19: ZnO nanostructures based on different time reaction through FESEM (Haque *et al.*, 2012)

Table 2.5: Summary of tests done with different variations in time (XRD, I-V Measurement, AFM and FESEM)

XRD		
Researchers	Parameter	Results
Ismail <i>et al.</i> , (2005)	Method : Hydrothermal Solution : $Zn(CH_3CO_2)_2 \cdot 2H_2O$ and NaOH Duration: 5-10 Hours	Plane: (101),(002), (100)
Shi <i>et al.</i> , (2010)	Method: Hydrothermal Solution: $ZnSO_4$ and Na_2CO_3 Duration: 6-12 Hours	Figure 2.13
Nagaraju <i>et al.</i> , (2010)	Method: Hydrothermal Solution: $ZnSO_4 \cdot 7H_2O$ and NaOH Duration: 6-24 Hours	Figure 2.14
I-V Measurement		
Amin & Willander, (2012)	Method: Hydrothermal Solution: Zn Precursors Duration: 6-8 Hours	Voltage Value = 1.52 V
Lira-Cantu & Krebs, (2006)	Method: Spin-Coated Solution: 2-Propanol, ZnAC and Diethanolamine Duration: 2 Hours	Table 2.4
AFM		
Nithya & Radhakrishnan, (2012)	Method : Coated by chemical bath technique Solution: $ZnCl_2$ and NaOH Duration: 30-150 minutes	Figure 2.15
Zhitao <i>et al.</i> , (2013)	Method: Hydrothermal Solution: $Zn(NO_3)_2$, HMTA and Distilled water. Duration: 1-12 Hours	Figure 2.16
Kamaruddin <i>et al.</i> , (2010)	Method: Sol-gel hydrothermal Solution: $Zn(NO_3)_2 \cdot 6H_2O$ and $C_6H_{12}N_4$ Duration: 5 Hours	Figure 2.17
FESEM		
Chen <i>et al.</i> , (2014)	Method: Hydrothermal Solution: $Zn(O_2CCH_3)_2$ and HMT Duration: 7 Hours	Nanoflowers and nanorods
Liu <i>et al.</i> , (2005)	Method: Solution Deposition Method Solution: $Zn(NO_3)_2 \cdot 6H_2O$ and HMT Duration: 1-5 Hours	Figure 2.18
Haque <i>et al.</i> , (2012)	Method: Uncovered Hydrothermal Solutions: $Zn(NO_3)_2 \cdot 6H_2O$ and HMT Duration: 60-240 Minutes	Figure 2.19

2.5 Effects of Different pH

Besides the varying factors of solutions and time allocations used in the hydrothermal process, different pH levels in solutions do effect the ZnO structurestoo. This fact is strengthened by the results of the research done by Musić *et al.*, (2005) on the size and properties of ZnO particles with effects from chemical synthesis. The $\text{Zn}(\text{CH}_3\text{COO})_2 \cdot 2\text{H}_2\text{O}$ is neutralised using hydrothermal techniques with different quantities of NH_4OH solution.

The pH of NaOH was adjusted from 11,12,13 to 14 in the research by Zhao, Li, & Lou, (2014). The formation of structures were different when NaOH pH was added. The illustration of the formation can be seen in Figure 2.20. When a solution that is alkalic with the pH of 11 was used, the microstructures were of hexagonal prism in shape with a diameter of 1 μm . Structure disk that has a diameter of 5 μm are shaped using the solution that is of pH 12. The addition of pH 13 forms spherical structures with 3-5 μm in diameter. The pH 14 solution of NaOH produced well flowers in 3D microstructures that resembled petals.

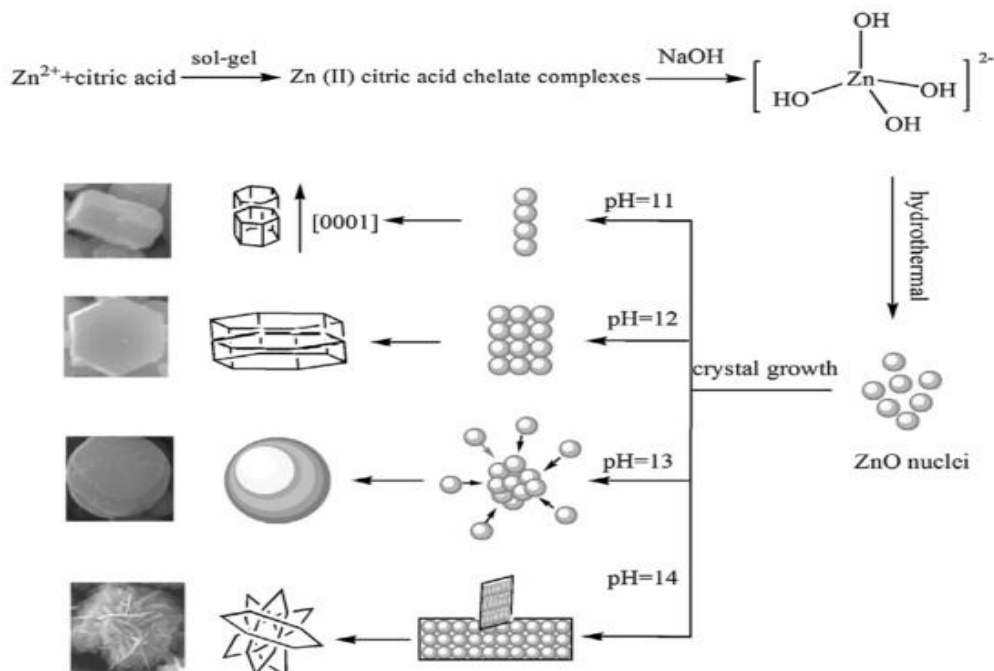


Figure 2.20: The formation of ZnO structures using the Hydrothermal technique in different pH NaOH solutions (Zhao *et al.*, 2014).

Research done by Bhat, Shrisha, & Naik, (2013) using the solvothermal method uses water and methanol as solvents. When using water as a solvent, the value of the alkaline solution is recorded at 8 and 12 pH, while when using methanol as a solvent, the solution of NaOH with 8 and 9 pH was produced. Even though the experiments were conducted with different pH values and solvents, the plane at (101) is still a favourite plane for ZnO. XRD results of this research are shown in Figure 2.21.

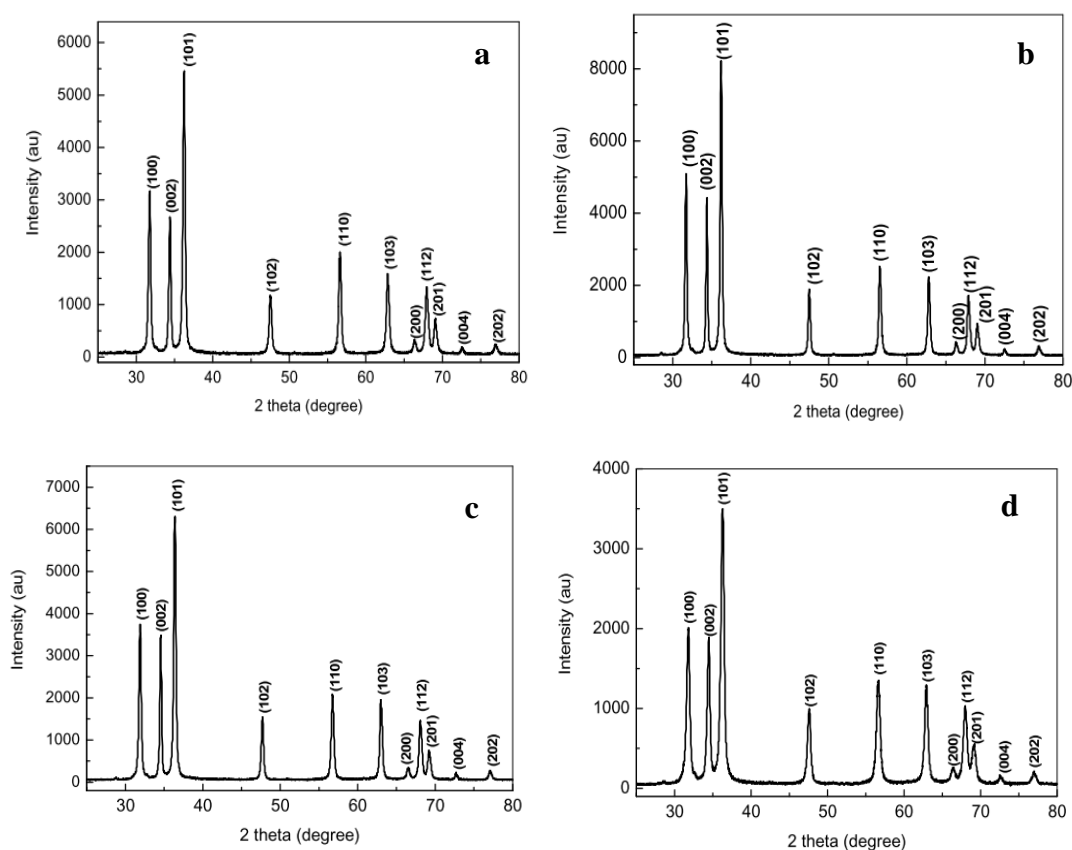


Figure 2.21: XRD patterns for ZnO nanostructures (a) water as solvent with pH = 8 (b) water as solvent with pH = 12 (c) methanol as solvent with pH = 8 (d) water as solvent with pH = 9 (Bhat *et al.*, 2013).

Based on the Figure 2.22, all the XRD patterns for all pH values are crystalline in nature with peaks corresponding at (100), (002), and (101) planes. The intensity of peaks increase with the increase of pH values. In this figure, the ZnO powder at pH 9 has the most crystalline structure because it has the most intense peaks. The intense of XRD peaks decreases at pH 10 and pH 11.

REFERENCES

- Amin, G., & Willander, P. M. (2012). *ZnO and CuO Nanostructures: Low Temperature Growth, Characterization, their Optoelectronic and Sensing Applications*. Department of Science and Technology, Physics and Electronics (Vol. PhD). Retrieved from <http://liu.diva-portal.org/smash/record.jsf?pid=diva2:515790>
- Baek, K. K., & Tuller, H. L. (1995). Electronic Characterization of ZnO/CuO heterojunctions. *Solid State Ionics*, 179-186.
- Baruah, S., & Dutta, J. (2009). Hydrothermal growth of ZnO nanostructures. *Science and Technology of Advanced Materials*, 10(1), 013001. doi:10.1088/1468-6996/10/1/013001
- Bang, S., Lee, S., Ko, Y., Park, J., Shin, S., Seo, H., & Jeon, H. (2012). Photocurrent detection of chemically tuned hierarchical ZnO nanostructures grown on seed layers formed by atomic layer deposition. *Nanoscale Research Letters*, 7(1), 290. doi:10.1186/1556-276X-7-290
- Baviskar, P. K., Tan, W., Zhang, J., & Sankapal, B. R. (2009). Wet chemical synthesis of ZnO thin films and sensitization to light with N3 dye for solar cell application. *Journal of Physics D: Applied Physics*, 42(12), 125108. doi:10.1088/0022-3727/42/12/125108
- Beard, M. C., Luther, J. M., & Nozik, A. J. (2014). The promise and challenge of nanostructured solar cells. *Nature Publishing Group*, 9(12), 951–954. doi:10.1038/nnano.2014.292
- Berruet, M., Pereyra, C. J., Mhlongo, G. H., Dhlamini, M. S., Hillie, K. T., Vázquez, M., & Marotti, R. E. (2013). Optical and structural properties of nanostructured ZnO thin films deposited onto FTO/glass substrate by a solution-based technique. *Optical Materials*, 35(12), 2721–2727. doi:10.1016/j.optmat.2013.08.018
- Bhat, S., Shrishya, B. V., & Naik, K. G. (2013). Synthesis of ZnO nanostructures by solvothermal method, 4(2), 61–70.
- Chen, J., Li, J., Xiao, G., & Yang. (2010). *J. Alloys Comp. Large-scale synthesis of uniform ZnO nanorods and ethanol gas sensors application*, 740-743.

- Chen, Y.-C., Cheng, H.-Y., Yang, C.-F., & Hsieh, Y.-T. (2014). Journal of Nanomaterials. *Investigation of the Optimal Parameters in Hydrothermal Methods for the Synthesis of ZnO Nanorods*.
- Choi, J. H., You, X., Kim, C., Park, J., & Pak, J. J. (2010). Power generating characteristics of zinc oxide nanorods grown on a flexible substrate by a hydrothermal method. *Journal of Electrical Engineering and Technology*, 5(4), 640–645. doi:10.5370/JEET.2010.5.4.640
- Chou, T. P., Zhang, Q., Fryxell, G. E., & Cao, G. Z. (2007). Hierarchically Structured ZnO Film for Dye-Sensitized Solar Cells with Enhanced Energy Conversion Efficiency. *Advanced Materials*, 19(18), 2588–2592. doi:10.1002/adma.200602927
- Dezfoolian, M., Rashchi, F., & Ravanbakhsh, A. (2014). Nano structured copper-zinc oxide thin film synthesis by anodic oxidation method in alkaline media. *Conference of Iranian Metallurgical Engineering and Iranian Foundryman*.
- Ekthammathat, N., Thongtem, S., Thongtem, T., & Phuruangrat, A. (2014). Characterization and antibacterial activity of nanostructured ZnO thin films synthesized through a hydrothermal method. *Powder Technology*, 254, 199–205. doi:10.1016/j.powtec.2014.01.010
- Ekthammathat, N., Thongtem, T., Phuruangrat, A., & Thongtem, S. (2013). Journal of Nanomaterials. *Photoluminescence of Hexagonal ZnO Nanorods Hydrothermally Grown on Zn Foils in KOH Solution with Different Values of Basicity*, 4.
- Fan, Z., & Lu, J. (2005). Zinc Oxide Nanostructured : Synthesis and Properties. *Journal of Nanoscience and Nanotechnology*, 1561-1573.
- Gomez, J. L., & Tigli, O. (2012). Zinc oxide nanostructures: from growth to application. *Journal of Materials Science*, 48(2), 612–624. doi:10.1007/s10853-012-6938-5
- Haque, R., Mandal, R. S., Islam, M. S., & Hossain, M. F. (2012). Nanostructured ZnO Thin Films by Uncovered Hydrothermal Method for Solar Cell Application, 98–100.
- Houng, B., Huang, C.-L., & Tsai, S.-Y. (2007). Effect of the pH on the growth and properties of sol-gel derived boron-doped ZnO transparent conducting thin film. *Journal of Crystal Growth*, 307(2), 328–333. doi:10.1016/j.jcrysgro.2007.07.001
- Huang, J., Yin, Z., & Zheng, Q. (2011). Applications of ZnO in organic and hybrid solar cells.
- International Zinc Association*. (2011). Retrieved 30 October, 2014, from Zinc Website: http://www.zinc.org/info/zinc_oxide_applications

- Ismail, a. a., El-Midany, a., Abdel-Aal, E. a., & El-Shall, H. (2005). Application of statistical design to optimize the preparation of ZnO nanoparticles via hydrothermal technique. *Materials Letters*, 59(14-15), 1924–1928. doi:10.1016/j.matlet.2005.02.027
- Kamaruddin, S. A., Sahdan, M. Z., Chan, K., Rusop, M., & Saim, H. (2010). SYNTHESIS AND CHARACTERIZATIONS OF ZINC OXIDE NANOSTRUCTURES Sinteza in karakterizacija nanostruktur cinkovega oksida, 40, 17–19.
- Kharisov, B. I., Kharissova, O. V., & Méndez, U. O. (2012). Microwave Hydrothermal and Solvothermal Processing of Materials and Compounds.
- Kołodziejczak-Radzimska, A., & Jesionowski, T. (2014). Zinc Oxide—From Synthesis to Application: A Review. *Materials*, 7(4), 2833–2881. doi:10.3390/ma7042833
- Komarneni, S. (2003). Nanophase materials by hydrothermal , microwave-hydrothermal and microwave-solvothermal methods, 85(12).
- Lai, Y., Meng, M., Yu, Y., Wang, X., & Ding, T. (2011). Photoluminescence and photocatalysis of the flower-like nano-ZnO photocatalysts prepared by a facile hydrothermal method with or without ultrasonic assistance. *Applied Catalysis B: Environmental*, 105(3-4), 335–345. doi:10.1016/j.apcatb.2011.04.028
- Li, Z., Huang, X., Liu, J., Li, Y., Ji, X., & Li, G. (2007). Growth and comparison of different morphologic ZnO nanorod arrays by a simple aqueous solution route. *Materials Letters*, 61(22), 4362–4365. doi:10.1016/j.matlet.2007.02.003
- Lira-Cantu, M., & Krebs, F. C. (2006). Hybrid solar cells based on MEH-PPV and thin film semiconductor oxides (TiO₂, Nb₂O₅, ZnO, CeO₂ and CeO₂-TiO₂): Performance improvement during long-time irradiation. *Solar Energy Materials and Solar Cells*, 90(14), 2076–2086. doi:10.1016/j.solmat.2006.02.007
- Liu, B., & Zeng, H. (2003). Journal of the American Chemical Society. *Hydrothermal synthesis of ZnO nanorods in the diameter regime of 50 nm*, 4430-4431.
- Liu, X., Jin, Z., Bu, S., Zhao, J., & Liu, Z. (2005). *Materials Letters. Effect of Buffer Layer on Solution deposited ZnO Films.*
- Mondal, S., Kanta, K. P., & Mitra, P. (2012). Preparation of ZnO film on p-Si and I-V characteristic of p-Si/n-ZnO. *Material Research.*
- Musić, S., Dragčević, D., Popović, S., & Ivanda, M. (2005). Mater. Lett. *Precipitation of ZnO particles and their properties.*, 2388-2393.

- Nagaraju, G., Ashoka, S., Chithaiah, P., Tharamani, C. N., & Chandrappa, G. T. (2010). Surfactant free hydrothermally derived ZnO nanowires, nanorods, microrods and their characterization. *Materials Science in Semiconductor Processing*, 13(1), 21–28. doi:10.1016/j.mssp.2010.02.002
- Ni, Y., Wei, X., Hong, J., & Ye, Y. (2005). Hydrothermal preparation and optical properties of ZnO nanorods. *Materials Science and Engineering: B*, 121(1-2), 42–47. doi:10.1016/j.mseb.2005.02.065
- Nithya, N., & Radhakrishnan, S. (2012). Effect of Thickness on the Properties ZnO Thin Films. *Pelagiaresearchlibrary.Com*, 3(6), 4041–4047. Retrieved from <http://www.pelagiaresearchlibrary.com/advances-in-applied-science/vol3-iss6/AASR-2012-3-6-4041-4047.pdf>
- Noriega, R., Rivnay, J., Goris, L., Kälblein, D., Klauk, H., Kern, K., ... Salleo, A. (2010). Probing the electrical properties of highly-doped Al:ZnO nanowire ensembles. *Journal of Applied Physics*, 107(7), 074312. doi:10.1063/1.3360930
- Pei, L. Z., Zhao, H. S., Tan, W., Yu, H. Y., Chen, Y. W., Fan, C. G., & Zhang, Q. F. (2010). Hydrothermal oxidization preparation of ZnO nanorods on zinc substrate. *Physica E: Low-Dimensional Systems and Nanostructures*, 42(5), 1333–1337. doi:10.1016/j.physe.2009.08.026
- Rafaie, H. a., Samat, N. a., & Nor, R. M. (2014). Effect of pH on the growth of zinc oxide nanorods using Citrus aurantifolia extracts. *Materials Letters*, 137, 297–299. doi:10.1016/j.matlet.2014.09.033
- Rani, S., Suri, P., Shishodia, P. K., & Mehra, R. M. (2008). Synthesis of nanocrystalline ZnO powder via sol-gel route for dye-sensitized solar cells. *Solar Energy Materials and Solar Cells*, 92(12), 1639–1645. doi:10.1016/j.solmat.2008.07.015
- Ridhuan, N. S., Razak, K. A., Lockman, Z., & Abdul Aziz, A. (2012). Structural and morphology of ZnO nanorods synthesized using ZnO seeded growth hydrothermal method and its properties as UV sensing. *PloS One*, 7(11), e50405. doi:10.1371/journal.pone.0050405
- Sagadevan, S. (2013). Recent trends on nanostructures based solar energy applications: A review. *Reviews on Advanced Materials Science*, 34(1), 44–61.
- Shariffudin, S. S., Salina, M., Herman, S. H., & Rusop, M. (2012). Effect of Film Thickness on Structural, Electrical, and Optical Properties of Sol-Gel Deposited Layer-by-layer ZnO Nanoparticles. *Transactions on Electrical and Electronic Materials*, 13(2), 102–105. doi:10.4313/TEEM.2012.13.2.102
- Shi, W. T., Gao, G., & Xiang, L. (2010). Synthesis of ZnO whiskers via hydrothermal decomposition route. *Transactions of Nonferrous Metals Society of China (English Edition)*, 20(6), 1049–1052. doi:10.1016/S1003-6326(09)60256-9

- Shinde, V. R., Gujar, T. P., & Lokhande, C. D. (2007). Studies on growth of ZnO thin films by a novel chemical method. *Solar Energy Materials and Solar Cells*, 91(12), 1055–1061. doi:10.1016/j.solmat.2007.02.017
- Segovia, M., Sotomayor, C., Gonzalez, G., & Benavente, E. (n.d.). *Zinc Oxide Nanostructured by Solvothermal Synthesis*.
- Shariffudin, S. S., Salina, M., Herman, S. H., & Rusop, M. (2012). Effect of Film Thickness on Structural, Electrical, and Optical Properties of Sol-Gel Deposited Layer-by-layer ZnO Nanoparticles. *Transactions on Electrical and Electronic Materials*, 13(2), 102–105. doi:10.4313/TEEM.2012.13.2.102
- Shi, W. T., Gao, G., & Xiang, L. (2010). Synthesis of ZnO whiskers via hydrothermal decomposition route. *Transactions of Nonferrous Metals Society of China (English Edition)*, 20(6), 1049–1052. doi:10.1016/S1003-6326(09)60256-9
- Tadatsugu, M. (2005). Semiconductor Science and Technology. *Transparent Conducting Oxide Semiconductor For Transparent Electrodes*.
- Tseng, Y., & Feng, Y. (n.d.). Fabrication and Morphology Control of ZnO Nanowires by Hydrothermal Method. *Tdx.Yuntech.Edu.Tw*. Retrieved from [http://tdx.yuntech.edu.tw/dmdocuments/Fabrication and Morphology Control of ZnO Nanowires by Hydrothermal Method.pdf](http://tdx.yuntech.edu.tw/dmdocuments/Fabrication%20and%20Morphology%20Control%20of%20ZnO%20Nanowires%20by%20Hydrothermal%20Method.pdf)
- Vijayan, T. A., Chandramohan, R., Valanarasu, S., Thirumalai, J., Venkateswaran, S., Mahalingam, T., & Srikumar, S. R. (2008). Optimization of growth conditions of ZnO nano thin films by chemical double dip technique. *Science and Technology of Advanced Materials*, 9(3), 035007. doi:10.1088/1468-6996/9/3/035007
- Wahab, R., Kim, Y.-S., & Shin, H.-S. (2009). Synthesis, Characterization and Effect of pH Variation on Zinc Oxide Nanostructures. *Materials Transactions*, 50(8), 2092–2097. doi:10.2320/matertrans.M2009099
- Yang, Z., Luan, C., Zhang, W., Liu, A., & Tang, S. (2008). Fabrication and optical properties of ZnO nanostructured thin films via mechanical oscillation and hydrothermal method. *Thin Solid Films*, 516(18), 5974–5980. doi:10.1016/j.tsf.2007.10.085
- Yangyang, Z., Manoj, K., Elias, K., & Goswami, D. (2012). Journal of Nanomaterials. *Synthesis, Characterization, and Applications of ZnO Nanowires*, 22.
- Yuan, Z., Yu, J., & Jiang, Y. (2011). Growth of diameter-controlled zno nanorod arrays by hydrothermal technique for polymer solar cell application. *Energy Procedia*, 12, 502–507. doi:10.1016/j.egypro.2011.10.067

- Zhang, K., Khadka, S., Nminibapiel, D., Tangirala, M., & Baumgart, H. (2013). ZnO Nanorods Grown on ZnO Seed Layer Derived by Atomic Layer Deposition Process. *ECS Meeting The Electrochemical Society*.
- Zhao, X., Li, M., & Lou, X. (2014). Sol–gel assisted hydrothermal synthesis of ZnO microstructures: Morphology control and photocatalytic activity. *Advanced Powder Technology*, 25(1), 372–378. doi:10.1016/j.appt.2013.06.004
- Zhitao, H., Sisi, L., Jinkui, C., & Yong, C. (2013). Controlled growth of well-aligned ZnO nanowire arrays using the improved hydrothermal method, 34(6), 1–6. doi:10.1088/1674-4926/34/6/063002
- Zhou, Q., Chen, W., Peng, S., & Zeng, W. (2014). Hydrothermal Synthesis and Acetylene Sensing Properties of Variety Low Dimensional Zinc Oxide Nanostructures. *The Scientific world Journal* .
- Zou, X., Liu, Y., Wei, C., Huang, Z., & Meng, X. (2014). Journal of Chemistry. *Electrodeposition Combination with Hydrothermal Preparation of ZnO Films and Their Applications in Dye Sensitized Solar Cell*, 5.